Abstract

In this paper, I work to find solutions to existing problems in compressed sensing of fMRI data. First, I study a wavelet-based algorithm and modify it to reconstruct data from subsampled Fourier space. Secondly, I study biased subsampling of fMRI data favoring lower frequencies. Ultimately, I find the modified wavelet-based algorithm to be an effective method of reconstruction for subsampled fMRI data, and I find the favored sampling of lower frequencies in Fourier space to reduce imaging errors and ultimately produce more accurate reconstructions.

1 Introduction

Compressed sensing has become an increasingly important aspect of signal processing, with applications ranging from medical imaging to ocean floor mapping. While sampling at the Nyquist rate (twice the maximum frequency of the signal), signal processing theory has shown that signals can be recovered exactly [6]. However, utilizing compressed sensing has great potential advantages as it allows effective signal recovery to occur with significantly fewer samples than the Nyquist limit would require. As such, signals can be processed faster and with greater efficiency with the use of compressed sensing. In general, compressed sensing has proven effective at reconstructing static 2D images, though its applications are being spread towards a variety of signal types.

In this paper, I examine the application of compressed sensing for fMRI, or functional magnetic resonance imaging. This is a particularly important application, as fMRI scans typically extract large amounts of data, which in turn requires a significant amount of time. Movement during an fMRI scan can distort the extracted images, which becomes a problem with patients who have difficulties restraining movement, such as small children. Hence, if one were able to extract the same amount of information in a shorter amount of time, both the clarity of images produced and the overall comfort of patients could be increased significantly. Furthermore, fMRI data is conducive to effective compressed sensing recovery, as the data is taken in Fourier space. We can hence extract our samples directly from Fourier space, and reconstruct an image from an inverse Fourier transform of our data. It is important to note that the method of sampling from Fourier space must be restricted when dealing with fMRI data. As fMRI data is taken in rows of Fourier space, we must sample out entire rows, rather than individual elements [1].

Recent research has shown that although reconstructions of fMRI scans using compressed sensing maintained 95% statistical correlation at 50% compression, i.e. retaining only 50% of the total data, the regression error over time deviated from normality, and the general linear model exhibited some bias [2]. The data also suggested these errors may have occurred as a result of the staircasing effects of the TV, or Total Variation, minimization algorithm used. I have now directed my efforts towards utilizing other methods of compressed sensing for fMRI data, both to see if a more effective algorithm could correct these errors in parameter estimates, and more generally to see if there is a way to produce faster, clearer images with compressed sensing.

2 Wavelet-Based Compressed Sensing

Recently, Cai, Dong, and Shen [3] have proposed a Wavelet-based image reconstruction, and have shown it to be very effective at removing Gaussian blur. In contrast with a Wavelet-based L1 regularization like

$$\inf_u ||\gamma \cdot Wu||_1 + \frac{1}{2}||Au - f||_2^2,$$

the proposed algorithm is able to produce images that both maintained smoothness and sharpness of edges by solving the following minimization problem:

$$\inf_{u,\Gamma} ||[\lambda \cdot Wu]_{\Gamma^C}||_2^2 + ||[\gamma \cdot Wu]_\Gamma||_1 + \frac{1}{2}||Au - f||_2^2. \tag{1}$$

Here Γ denotes the jump set, or the distinguishing edges of the image, and W denotes the wavelet transform. The algorithm works by breaking a single image into piecewise smooth composite images. The $||[\gamma \cdot Wu]_\Gamma||_1$ term minimizes the oscillation of the jump set in the image, while the $||[\lambda \cdot Wu]_{\Gamma^C}||_2^2$ term minimizes oscillation away from the jump set. This idea is similar to the Mumford-Shah functional [5].The above minimization problem is solved as an alternating scheme. We fix Γ and minimize (1) with respect to u and alternate this with fixing u and minimizing (1) with respect to Γ until the scheme converges.

At iteration k, given Γ^{k-1}, u^k is found by iterating the following Split Bregman algorithm with $d^0 = b^0 = 0$ for $j = 1, 2, ...$

$$\begin{aligned} u^{k,j} &= \text{argmin}_u \frac{1}{2}||Au - f||_2^2 + \frac{\mu}{2}||Wu - d^{j-1} + b^{j-1}||_2^2 \qquad (2)\\ d^j &= \text{argmin}_d ||[\lambda \cdot d]_{(\Gamma^{k-1})^C}||_2^2 + ||[\gamma \cdot d]_{(\Gamma^{k-1})}||_1 + \frac{\mu}{2}||d - Wu^{k,j} - b_{j-1}||_2^2 \\ b^j &= b^{j-1} + (Wu^{k,j} - d^j) \end{aligned}$$

Given the efficacy of this algorithm, we then seek to modify the algorithm to utilize subsampling of Fourier space, as is done if fMRI compression, rather than blurring, as the type of image distortion. To do so, we need only modify the $\frac{1}{2}||Au - f||_2^2$ term. We first define the discrete Fourier transform of $u \in \mathbb{C}^{N \times N}$ by

$$Fu = \frac{1}{N}\Psi u \Psi,$$

where $\Psi = \left(e^{\frac{-2ikl\pi}{N}}\right)_{k,l}$. Notice that we can decompose Ψ into real and imaginary parts as follows:

$$\Psi = B - iC,$$

where $B = \cos\left(\frac{2kl\pi}{N}\right)_{k,l}$ and $C = \sin\left(\frac{2kl\pi}{N}\right)_{k,l}$. With these definitions, the inverse Fourier transform is given by

$$F^{-1}u = \frac{1}{N}\Psi^* u \Psi^*,$$

where Ψ^* denotes the conjugate transpose of A.

We define $S \in \mathbb{R}^{k\times N}$, a subsampled identity matrix, to be a subsampling matrix and $g = SFu_0$ to be the original subsampled Fourier data, i.e. u_0 is the original image data, $u_0 \in \mathbb{R}^{N\times N}$. Hence, to modify the algorithm for subsampling of Fourier space, we must alter the $\frac{1}{2}||Au - f||_2^2$ term to become of the form $\frac{1}{2}||SFu - g||_2^2$. If we make this substitution in (2) and solve for $u^{k,j}$ via the Euler-Lagrange equations, it is difficult to impose the constraint that $u^{k,j}$ should be real-valued. In order to impost this constraint, we take an alternative approach. First, we multiply both terms in the fidelity by S^T, making both terms $N \times N$ matrices, so

$$||SFu - g||_2^2 = ||S^T SFu - S^T g||_2^2.$$

By Plancheral's theorem, $||F^{-1}u||_2^2 = ||u||_2^2$, and hence

$$\begin{aligned} ||S^T SFu - S^T g||_2^2 &= ||F^{-1}S^T SFu - F^{-1}S^T g||_2^2 \\ &= ||\phi u - f||_2^2, \end{aligned}$$

where $\phi = F^{-1}S^T SF$ and $f = F^{-1}S^T g$, $f \in \mathbb{C}^{N\times N}$. Using our definitions of Fourier transforms,

$$\begin{aligned} \phi u &= F^{-1}S^T SFu \\ &= F^{-1}(S^T S(\frac{1}{N}AuA)) \\ &= \frac{1}{N^2}A^* S^T SAuAA^* \\ &= \frac{1}{N}A^* S^T SAu \\ &= \frac{1}{N}(B - iC)^* S^T S(B - iC)u \\ &= \frac{1}{N}(B + iC)S^T S(B - iC)u \\ &= \frac{1}{N}(BS^T SB + CS^T SC)u + i\frac{1}{N}(CS^T SB - BS^T SC)u \\ &= \phi_R u + i\phi_I u, \end{aligned}$$

where ϕ_R and ϕ_I are both real-valued matrices. Note for a matrix $A \in \mathbb{C}^{N\times N}$,

$$\begin{aligned}||A||_2^2 &= \sum_{k=1}^{N}\sum_{l=1}^{N}|A_{k,l}|^2 \\ &= \sum_{k=1}^{N}\sum_{l=1}^{N} Re(A_{k,l})^2 + Im(A_{k,l})^2 \\ &= ||Re(A)||_2^2 + ||Im(A)||_2^2,\end{aligned}$$

and hence

$$||\phi u - f||_2^2 = ||\phi_R u - Re(f)||_2^2 + ||\phi_I u - Im(f)||_2^2.$$

Hence, to modify the algorithm for subsampling of Fourier space, we must change the $\frac{1}{2}||Au - f||_2^2$ term to

$$\tfrac{1}{2}||\phi_R u - Re(f)||_2^2 + \tfrac{1}{2}||\phi_I u - Im(f)||_2^2,$$

and thus the overall minimization problem is

$$\min_u \tfrac{1}{2}||\phi_R u - Re(f)||_2^2 + \tfrac{1}{2}||\phi_I u - Im(f)||_2^2 + \tfrac{\mu}{2}||Wu - d^{j-1} + b^{j-1}||_2^2,$$

where the $\frac{\mu}{2}||Wu - d^{j-1} + b^{j-1}||_2^2$ term accounts for the wavelet transform and utilization of the jump set, and we set $h = d^{j-1} + b^{j-1}$. To solve this minimization, we derive the corresponding Euler-Lagrange equations. If u minimizes E, then for every vector $v \in \mathbb{R}^{N\times N}$

$$E(u) \leq E(u + tv) \text{ for all } t \in \mathbb{R},$$

so $E(u + tv)$ will have a minimum at $t = 0$. Thus, to minimize E, we set

$$\frac{d}{dt}\Big|_{t=0} \frac{1}{2}||\phi_R(u + tv) - Re(f)||_2^2 + \frac{1}{2}||\phi_I(u + tv) - Im(f)||_2^2 + \frac{\mu}{2}||W(u + tv) - h||_2^2 = 0.$$

And thus we have

$$\begin{aligned}0 &= \langle \phi_R u - Re(f), \phi_R v\rangle + \langle \phi_I u - Im(f), \phi_I v\rangle + \langle Wu - h, Wv\rangle \\ &= \langle \phi_R^T(\phi_R u - Re(f)) + \phi_I^T(\phi_I u - Im(f)) + \mu u - \mu W^T h, v\rangle.\end{aligned}$$

This equation holds true for every matrix $v \in \mathbb{R}^{N\times N}$, and hence

$$0 = \phi_R^T(\phi_R u - Re(f)) + \phi_I^T(\phi_I u - Im(f)) + \mu u - \mu W^T h.$$

Gathering u terms,

$$(\phi_R^T\phi_R + \phi_I^T\phi_I + \mu I)u = \phi_R^T Re(f) + \phi_I^T Im(f) + \mu W^T h.$$

Solving for u

$$u = (\phi_R^T\phi_R + \phi_I^T\phi_I + \mu I)^{-1}(\phi_R^T Re(f) + \phi_I^T Im(f) + \mu W^T h).$$

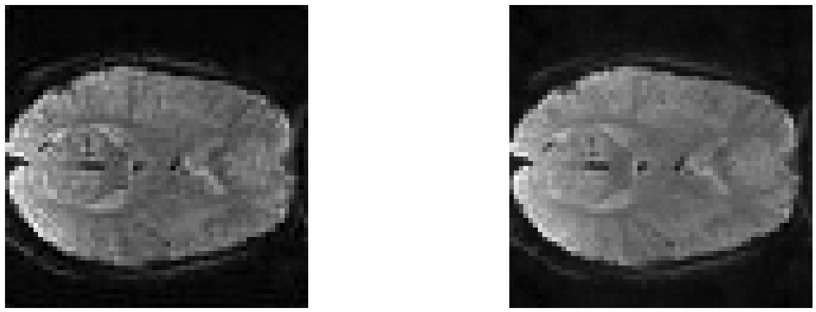

(a) (b)

Figure 1: Original Image (a) and reconstructed image (b) at 70% compression. Some overall smoothing has occurred, but important sharpness of edges has been preserved.

Hence, the overall Split Bregman algorithm becomes

$$u^{k,j} = \text{argmin}_u \frac{1}{2}||\phi_R u - Re(f)||_2^2 + \frac{1}{2}||\phi_I u - Im(f)||_2^2 + \frac{\mu}{2}||Wu - d^{j-1} + b^{j-1}||_2^2$$
$$d^j = \text{argmin}_d ||[\lambda \cdot d]_{(\Gamma^{k-1})^C}||_2^2 + ||[\gamma \cdot d]_{(\Gamma^{k-1})}||_1 + \frac{\mu}{2}||d - Wu^{k,j} - b_{j-1}||_2^2$$
$$b^j = b^{j-1} + (Wu^{k,j} - d^j)$$

Overall, the results were positive. Figures 1 and 2 show some sample reconstructions using this algorithm, along with a visualization of the calculated jump set. The PSNR for an image with 70% compression using this algorithm was 29.2711, while the PSNR for an image with 50% compression was 27.7383. Though some significant smoothing has occurred, the edges are well maintained and the overall structure of the image is reasonably well preserved. These PSNR values are similar to those of TV reconstructions, which average around 30, though by adjusting the gamma and lambda parameters it may be possible to obtain even higher PSNR values. This illuminates a drawback of the algorithm, in that the parameters are difficult to assign for a given reconstruction, and hence a good direction for future research would be to find a method for obtaining ideal parameter values for a given reconstruction.

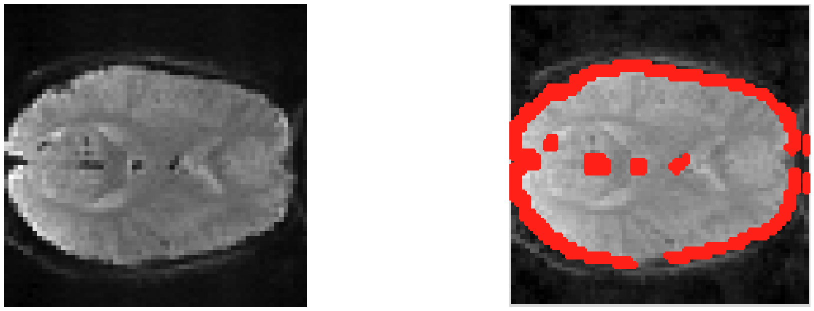

(a) (b)

Figure 2: Reconstructed image (a) at 50% compression and jump set (b) of reconstruction.

3 Biased Subsampling

My second area of research centered around different methods of subsampling in TV, or total variation, minimization, particularly in biasing the sampling towards lower-frequency samples. Prior research has shown that subsampling images to favor lower frequencies is able to produce images that are both clearer and lack some of the image errors caused due to sampling higher frequencies, all while maintaining the criterium required in compressed sensing theory[4]. This is because natural images tend to have more lower frequency and fewer higher frequency components in Fourier space, i.e. most of the Fourier values for high frequencies are 0. As such, if we favor lower frequencies, we may be better able to obtain a more accurate reconstruction. Though the effectiveness of biased sampling of individual pixels has been shown, when working with fMRI data, we must sample rows of Fourier space, as this is how fMRI data is gathered[1].

TV minimization solves the following minimization problem:

$$\hat{x} = \text{argmin}_x ||x||_{TV} \text{ s.t. } ||M(x) - y||_2 \leq \epsilon,$$

where $M = SF$, the subsampled Fourier transform. The directional derivatives x_h and x_v are defined as follows:

$$x_v : \mathbb{C}^{d^2} \to \mathbb{C}^{(d-1)\times d}, \quad (x_h)_{j,k} = x_{j+1,k} - x_{j,k}$$

$$x_h : \mathbb{C}^{d^2} \to \mathbb{C}^{d\times(d-1)}, \quad (x_v)_{j,k} = x_{j,k+1} - x_{j,k}$$

The discrete gradient transform is defined as follows:

$$((\nabla x)_{j,k,1}, (\nabla x)_{j,k,2}) := \begin{cases} ((x_v)_{j,k}, (x_h)_{j,k}) : & 1 \leq j,k \leq d-1 \\ (0, (x_h)_{j,k}) : & j = n, 1 \leq k \leq d-1 \\ ((x_v)_{j,k}, 0) : & k = n, 1 \leq j \leq d-1 \\ (0,0) : & j = k = d \end{cases}$$

(a) (b) (c)

Figure 3: Reconstruction (a) at 50% compression with no bias, reconstruction (b) at 50% compression with low bias, and reconstruction (c) at 50% compression with high bias.

And thus the TV norm is defined:

$$\|x\|_{TV} := \sum_{j,k=1}^{d} \left((\nabla x)_{j,k,1}^2 + (\nabla x)_{j,k,2}^2 \right)^{1/2}. \quad (3)$$

Utilizing the l1 magic package, I performed 100 reconstructions at 50% compression, i.e. retaining half of the available signals. I then split the reconstructions into three groups: No Bias, Low Bias, and High Bias. In the No Bias group, the rows were subsampled randomly from Fourier space. In the Low Bias group, the lowest frequencies had an 80% probability of being sampled, while the highest frequencies had a 20% probability. Between the lowest and highest frequencies, the likelihood of being sampled was linear from 80% to 20%. For the High Bias group, the lowest frequencies had a 90% probability of being sampled, while the highest frequencies had a 10% probability. Again, between the lowest and highest frequencies, the probability of being sampled was linear from 90% to 10%.

The results indicate the effectiveness of favoring lower-frequency samples (Fig 3, Fig 4, Fig 5, Table 1). Without bias, at 50% compression, the PSNR value given is 30.2693. With low bias, the PSNR value is 31.1782, and with high bias the PSNR value is 32.0792. Hence, we can see a correlation with higher bias towards lower-frequency samples and an increase in PSNR values. Furthermore, using the L^∞ norm, the average difference between the original and reconstructed image is lower for a higher bias, suggesting that higher levels of bias correspond to more accurate reconstructions.

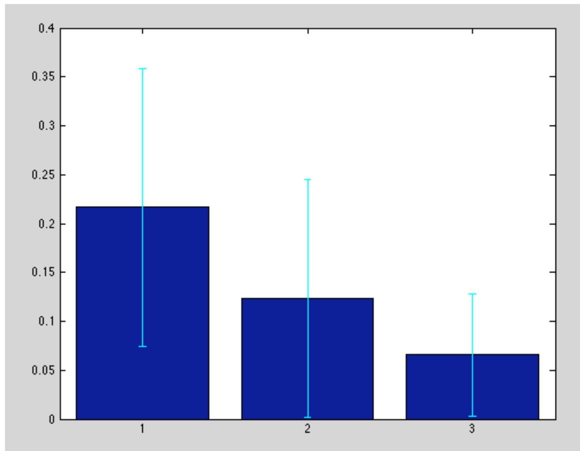

Figure 4: Average difference using the L^∞ norm between original and reconstructed image for no bias (column 1), low bias (column 2), and high bias (column 3) along with standard deviation of values.

	No Bias	Low Bias	High Bias
PSNR	30.2693	31.1782	32.0792

Table 1: Peak Signal-to-Noise Ratio (PSNR) values for No Bias, Low Bias, and High Bias reconstructions at 50% compression. The ratio values are higher for higher amounts of bias, suggesting a more accurate reconstruction.

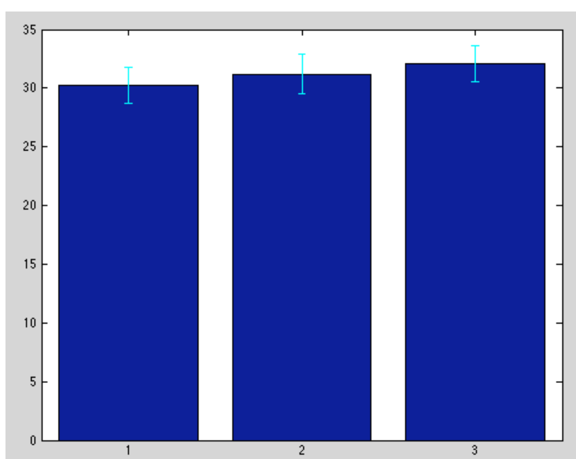

Figure 5: PSNR values for no bias (column 1), low bias (column 2), and high bias (column 3) reconstructions at 50% compression, along with standard deviation of values.

4 Discussion

Ultimately, I have effectively utilized several aspects of compressed sensing for fMRI data. The Cai, Dong, and Shen algorithm has now been shown to be an effective method of image recovery not only for blurred images, but also images that have been subsampled from Fourier space. Hence, it is possible that this algorithm could be utilized in the world of fMRI and MRI research, as it has the potential to reconstruct high quality images from subsampled data, and it does so relatively quickly. A direction for future research would be to see the effects on the normality of errors and bias in the generalized linear model, as the staircasing effects of TV minimization could have been taken care of.

Furthermore, I have shown the efficacy of subsampling from Fourier space with a bias towards lower-frequency samples. Again, this can be useful for fMRI and MRI research, because it provides a solution to some of the imaging errors that arise when subsampling randomly from Fourier space. A direction for future research in this respect would be to extract data over a large quantity of natural images to see if an overall natural bias towards certain frequencies is present. If this were the case, one could potentially sample data with respect to this ideal bias to produce even stronger reconstructions.

5 Acknowledgements

I would like to thank Jian-Feng Cai, Bin Dong, and Zuowei Shen for providing their code along with their paper. I would also like to thank Deanna Needell for providing her code on compressed sensing reconstruction with TV minimization. Finally, I would like to thank Jeff Calder for all his help as I researched and wrote my thesis.

References

[1] Amir A. Shafie Abiodun M. Aibinu, Momoh J. E. Salami and Athaur Rahman Najeeb. MRI reconstruction using discrete fourier transform: A tutorial. *World Academy of Science, Engineering and Technology*, 42, 2008.

[2] Aprineh Asadoorian, Christian Ayala, Ryan McCarthy, Jessica Nadalin, and Susannah Shoemaker. Compressed sensing impacts the statistical inferences made from fmri. *in preparation*, 2014.

[3] Bin Dong Jian-Feng Cai and Zuowei Shen. Image restoration: A wavelet frame based model for piecewise smooth functions and beyond.

[4] Felix Krahmer and Rachel Ward. Stable and robust sampling strategies for compressive imaging. *CoRR*, abs/1210.2380, November 2012.

[5] David Mumford and Jayant Shah. Optimal approximations by piecewise smooth functions and associated variational problems. *Communications on Pure and Applied Mathematics*, 42(5):577–685, 1989 1989.

[6] Deanna Needell and Rachel Ward. Stable image reconstruction using total variation minimization. *IEEE Transactions on Image Processing*, 22:3941–3949, 2013.